Critical Assessment of Pulse Annealing

N. Ghoniem and G. Kulcinski

March 1977

UWFDM-199

FUSION TECHNOLOGY INSTITUTE

UNIVERSITY OF WISCONSIN

MADISON WISCONSIN

Critical Assessment of Pulse Annealing

N. Ghoniem and G. Kulcinski

Fusion Technology Institute
University of Wisconsin
1500 Engineering Drive
Madison, WI 53706

http://fti.neep.wisc.edu

March 1977

UWFDM-199

Critical Assessment of Irradiation Pulse Annealing in Metals

N. Ghoniem
G. Kulcinski

March 1977

UWFDM-199

Fusion Technology Program
Nuclear Engineering Department
University of Wisconsin
Madison, Wisconsin 53706

Table of Contents

I. Introduction

Previous steady state rate theory models of void swelling in irradiated metals have provided valuable insight into the parameters that effect this phenomenon.[1,2] A recent expansion of the steady state theory to account for the dynamical aspects of the developing microstructure has also provided an insight into the behavior of metals during pulsed irradiation.[3] This Fully Dymamic Rate Theory (FDRT) has indicated that there may be a greatly reduced growth rate of voids during certain pulsed irradiation conditions. A key requirement of the FDRT is to accurately describe the annealing behavior of voids between pulses in order to ascertain whether this overall shrinkage is more or less than the growth due to the irradiation pulse. This paper focuses on this particular aspect and investigates the major parameters that influence the annealing kinetics of voids.

II. Theory

The time rate of change of a void of radius R_c in a metal is given by (3):

$$\frac{dR_c}{dt} = \{D_v C_v - D_i C_i - D_v C_v^e \exp\{(\frac{2\gamma}{R_c} - Pg\,(R_c, N_g))\,\frac{\Omega}{kT}\}/R_c \qquad (1)$$

where,

D_v = vacancy diffusion coefficient

D_i = interstitial diffusion coefficient

C_v = vacancy concentration in the matrix (at./at.)

C_i = interstitial concentration in the matrix (at./at.)

$C_v^e = \exp(-E_v^f/kT)$

= thermal equilibrium vacancy concentration (at./at.)

γ = surface energy (eV/cm^2)

E_v^f = vacancy formation energy (eV)

k = Boltzmann's constant ($eV/^oK$)

Ω = atomic volume (cm^3)

$$P_g(R_c, N_g) = \frac{3N_g kT}{4\pi(R_c^3 - 3b_v N_g/4\pi)} \qquad (2)$$

= gas pressure (eV/cm^3)

b_v = Van Der Waal's constant

N_g = number of gas atoms in the void.

While the time rate of change of a dislocation loop of radius $R_{i\ell}$ is given by [3]:

$$\frac{dR_{i\ell}}{dt} = \{D_i C_i Z_i - D_v C_v Z_v + D_v Z_v C_v (R_{i\ell})\}/b \quad (3)$$

where,

b = Burger's vector

Z_i = dislocation loop bias to interstitials

Z_v = dislocation loop bias to vacancies

$C_v(R_{i\ell})$ = equilibrium concentration of vacancies at the edge of an interstitial dislocation loop

$$= C_v^e \exp - \left(\frac{\{\gamma_{sf}+F_{e\ell}(R_{i\ell})\}b^2}{kT}\right) \quad (4)$$

and

$$F_{e\ell}(R_{i\ell}) = \frac{\mu b^2}{(1-\nu)4\pi(R_{i\ell}+b)} \ell n \left(\frac{R_{i\ell}+b}{b}\right) \quad (5)$$

where,

γ_{sf} = stacking fault energy, eV cm^{-2}

$F_{e\ell}(R_{i\ell})$ = elastic energy of a dislocation loop of radius $R_{i\ell}$, eV cm^{-2}

μ = shear modulus, eV cm^{-3}

ν = Poisson's ratio.

During irradiation, the vacancy and interstitial concentrations are determined by balancing the production and removal rates either by existing sinks or

by mutual recombination between point defects. If there is no production of point defects, their concentrations will be the thermal equilibrium concentrations for the annealing of voids. In between pulses, Equation (1) takes the simple form:

$$\frac{dR_c}{dt} = - D_v C_v^e \{\exp\left(\frac{2\Omega\gamma}{R_c kT}\right) - 1\}/R_c \ , \qquad (6)$$

provided that the void contains no gas atoms and that straight dislocations or grain boundaries are the dominant source/sink of thermal vacancies.

Also, Equation (3) takes the simple form:

$$\frac{dR_{i\ell}}{dt} = - D_v C_v^e \{1 - \exp\left(\frac{-\{\gamma_{sf}+F_{e\ell}(R_{i\ell})\}b^2}{kT}\right)\} \ . \qquad (7)$$

From Equations (6) and (7), it is clear that during the time between pulses, voids emit vacancies to the surrounding matrix reducing their size, while interstitial loops receive an excess flux of vacancies which also reduces their size.

III. Application of the Computer Code TRANSWELL to Annealing Studies in Metals

The computer code TRANSWELL[4] was constructed from the FDRT to study the response of metals during steady state or pulsed irradiation. However, the code is also flexibile enough to allow performing annealing studies on metals. The present work focuses on the accuracy of the bulk-diffusion limited model used in the computer code TRANSWELL and compares the calculated results with experimental findings.[5,6,7]

In a number of experiments, individual shrinkage curves were obtained for a number of voids at each temperature. This allowed the isolation of a few factors that affect void shrinkage, and that information was used to directly verify Equation (6).

Westmacott et al.[6] performed a void annealing experiment on Al in the temperature range 150-200°C. Voids were first produced by quenching, and Transmission Electron Microscope has been used to investigate the thermal stability of these voids. Assuming an activation energy of ~ 1.3 eV they estimated the surface energy to be γ_s = 1140 ± 200 ergs.

Volin and Balluffi[5] conducted another void annealing experiment on Al in the temperature range 85 to 209°C. Assuming a surface energy of 1500 ergs/cm^2 they estimated an activation energy of ~ 1.31 eV.

We have used the TRANSWELL code to simulate the annealing of voids in Al using the parameters listed in Table (1). The anneal was preceded by a very small amount of damage with the following characteristics;

pulse width = 10^{-8} seconds

pulse period = 1 hr - 30 hr depending on the temperature

production rate of point defects during the pulse = 5 dpa/sec

production rate of point defects after the pulse = 0. dpa/sec.

This approach is used for two purposes. The first goal is to simulate annealing experiments that actually have been done.[5,6] The second is to study pulse annealing of an existing void microstructure during the irradiation conditions typical of a laser fusion reactor.[8] From annealing point of view, the initial single irradiation pulse does not increase the initial void or loop radii significantly.

TABLE (1)

Parameters Used for Annealing Calculations in Aluminum

E_v^m(eV)	= 0.57	(9)
E_v^f(eV)	= 0.65 - 0.665 *	
D_v^o(cm^2/sec)	= 0.045	(9)
γ(ergs/cm^2)	= 1000 *	
b (Å)	= 2.32	(5)
Ω(cm^3)	= 1.25×10^{-23}	(5)
C_v^e(at./at.) at 126°C	= 6.159×10^{-9} *	
C_v^e(at./at.) at 175°C	= 3.302×10^{-8} *	

* These calculations

IV. Comparison of the Diffusion Model to Experiments

The presence of a void inside a crystal introduces an additional surface so that the surface energy γ provides a driving force to eliminate the void. Annealing at temperatures high enough to permit self-diffusion causes the voids to shrink by emitting vacancies. The energy of a void, radius R_c, is reduced by an amount $(\frac{2\gamma\Omega}{R_c})$ per vacancy emitted. This leads to a concentration gradient of vacancies between the void and the vacancy sinks. In thin foils the foil surfaces are often perfect sinks for vacancies and are thus able to maintain the vacancy concentration away from the voids at the thermal equilibrium level. In bulk samples these vacancies can go to other internal sinks including other voids.

Fig. (1) shows the results of the TRANSWELL Computer Code simulations on the annealing of a 152 $\mathring{A}$ void in Al at 126°C. This is compared with Volin and Balluffi experiment. A marked agreement between experimental and computer simulation values is obtained with a surface energy of γ = 1000 ergs/cm^2 and a vacancy formation energy E_v^f = 0.645 eV. Figure (2) shows the annealing behavior at a higher temperature consistent with the work of Westmacott et al. (175°C). Within the limits of experimental accuracy, good agreement between the TRANSWELL results and the experimental results is achieved. Again values of γ = 1000 ergs/cm^2 and E_v^f = 0.665 eV are found to produce good agreement. It is noted that the void anneals out about 30 times faster at the high temperature than at the lower temperature.

Neutron irradiated Aluminum[7] showed a slower annealing behavior than quenched Aluminum. There are numerous factors that could affect annealing kinetics. Those factors are void gas content, a transmutation modified surface energy, stress state of the sample, and the irradiation produced microstructure. Due to the importance of this inter-pulse annealing in

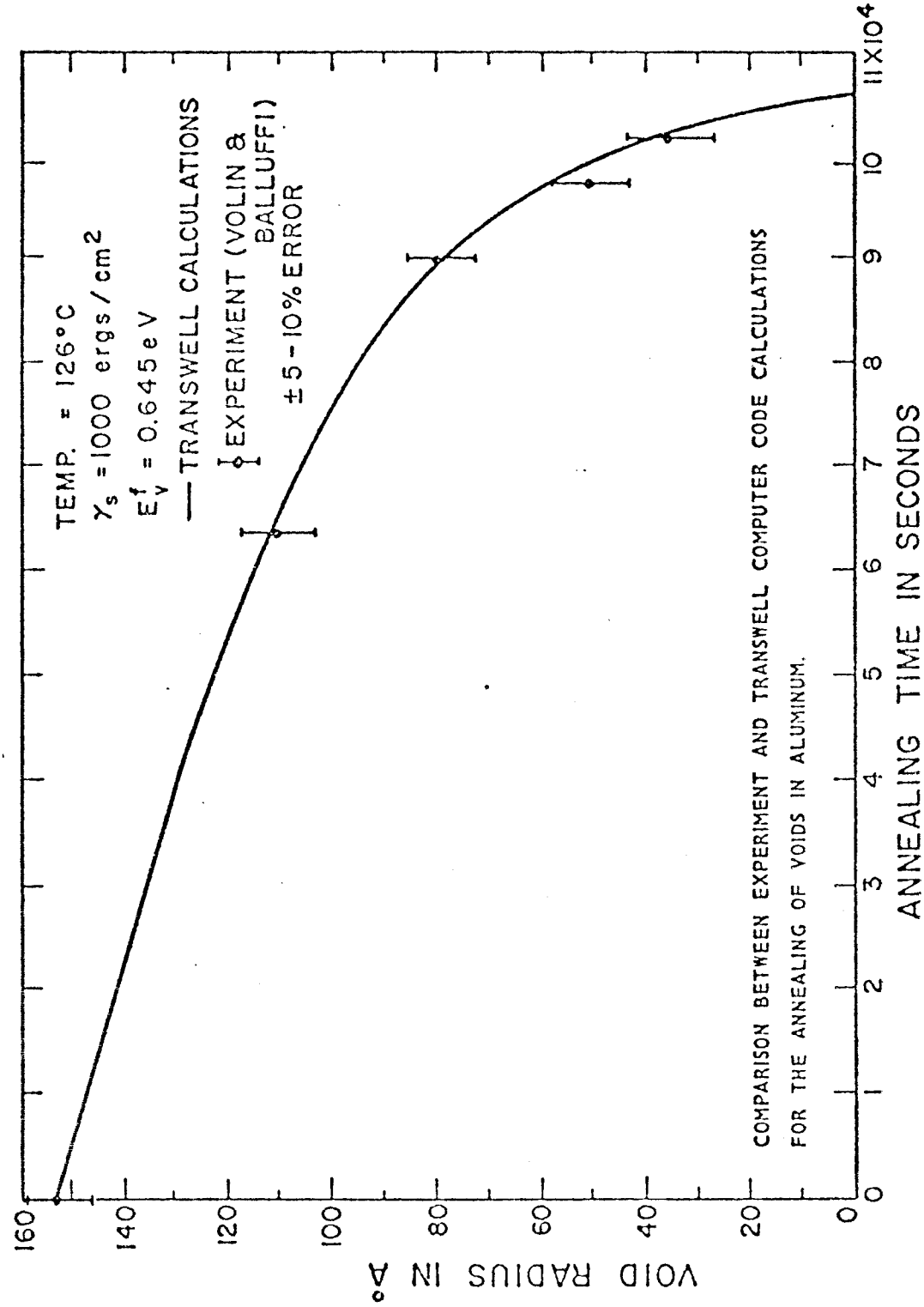
TEMP. = 126°C
γ_s = 1000 ergs / cm^2
E_v^f = 0.645 eV
TRANSWELL CALCULATIONS
EXPERIMENT (VOLIN & BALLUFFI)
±5-10% ERROR
COMPARISON BETWEEN EXPERIMENT AND TRANSWELL COMPUTER CODE CALCULATIONS
FOR THE ANNEALING OF VOIDS IN ALUMINUM.
VOID RADIUS IN Å
ANNEALING TIME IN SECONDS
0
20
40
60
80
100
120
140
160
1
2
3
4
5
6
7
8
9
10
11X10^4

FIG. 1

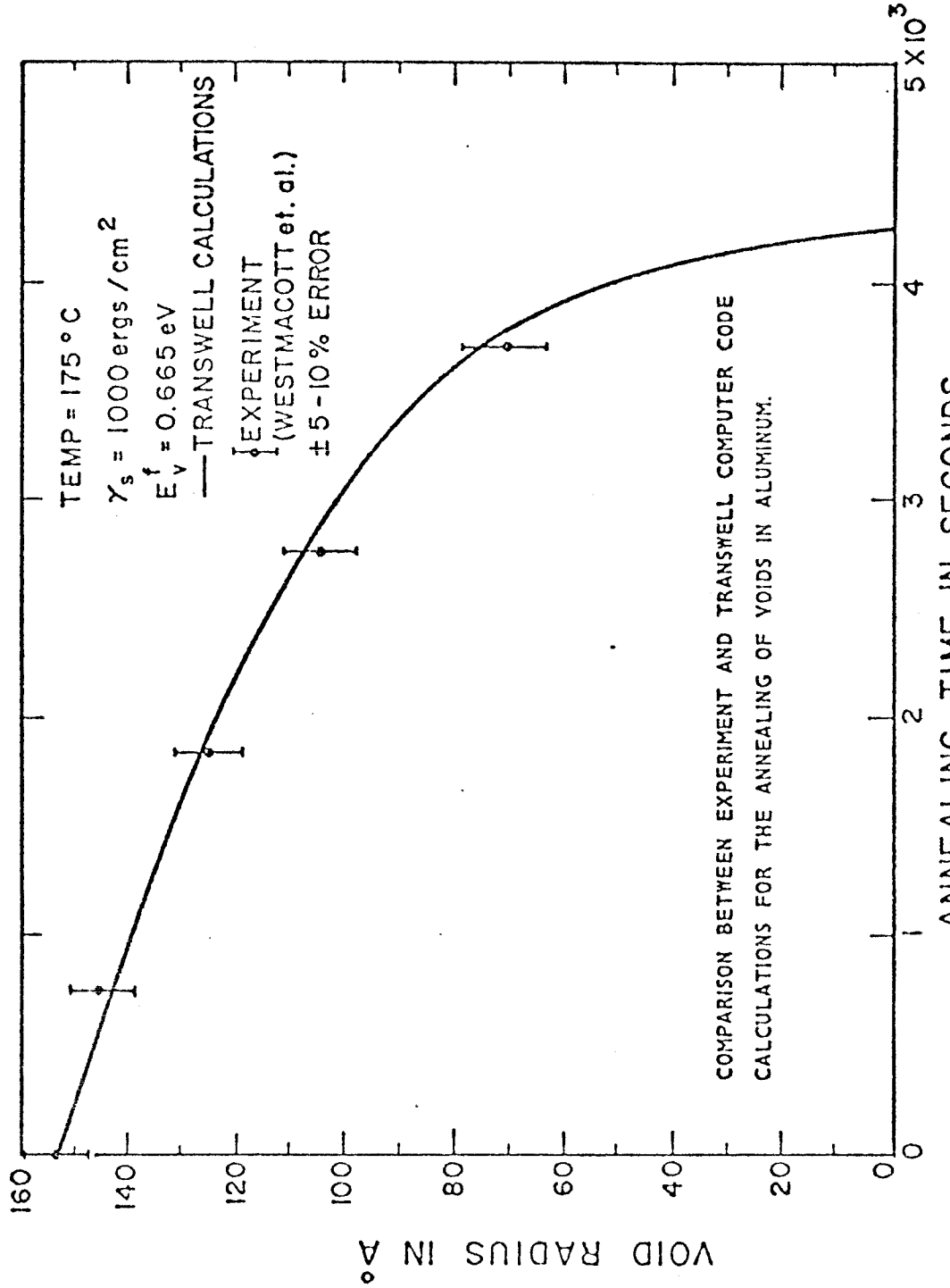
TEMP = 175 ° C
γ_s = 1000 ergs / cm^2
E_v^f = 0.665 eV
TRANSWELL CALCULATIONS
EXPERIMENT (WESTMACOTT et. al.)
± 5 - 10 % ERROR
COMPARISON BETWEEN EXPERIMENT AND TRANSWELL COMPUTER CODE CALCULATIONS FOR THE ANNEALING OF VOIDS IN ALUMINUM.
VOID RADIUS IN Å
ANNEALING TIME IN SECONDS
0
20
40
60
80
100
120
140
160
1
2
3
4
5 X 10^3

FIG. 2

Pulsed Systems, we will study the sensitivity of annealing kinetics to those factors in more detail in the next section.

V. Sensitivity of Annealing Kinetics to Material Parameters

The theoretical diffusion model is shown to be successful in predicting the annealing behavior of voids in the simplest case. A variety of important conditions are studied to understand their individual effects on the thermal void annealing phenomenon.

(a) Temperature

Figures (1) and (2) show the great sensitivity of void annealing to temperature. It is also shown that the void radius versus time curve is almost linear for the first stages of the annealing time. However, it becomes heavily non-linear as the void size decreases. This means that smaller size voids anneal out much faster than large size voids.

(b) Surface Energy

The value of void/matrix surface energy is known to have a great effect on calculated void nucleation rates under irradiation. Figure (3) shows the effect of changing the surface energy on annealing kinetics. It is noticed that quite large changes in the surface energy do not affect substantially the annealing kinetics in the early stages.

(c) Cavity Gas Content

Cavities in neutron irradiated aluminum showed slower annealing behavior than quenched in voids.[7] This behavior was attributed to the presence of gas atoms in the cavities. Using Van der Waal's gas equation (2), the annealing kinetics of a 152 $\mathring{A}$ cavity is studied in figure (4). It is observed that annealing behavior becomes slower as the number of He gas atoms is increased in the cavity.

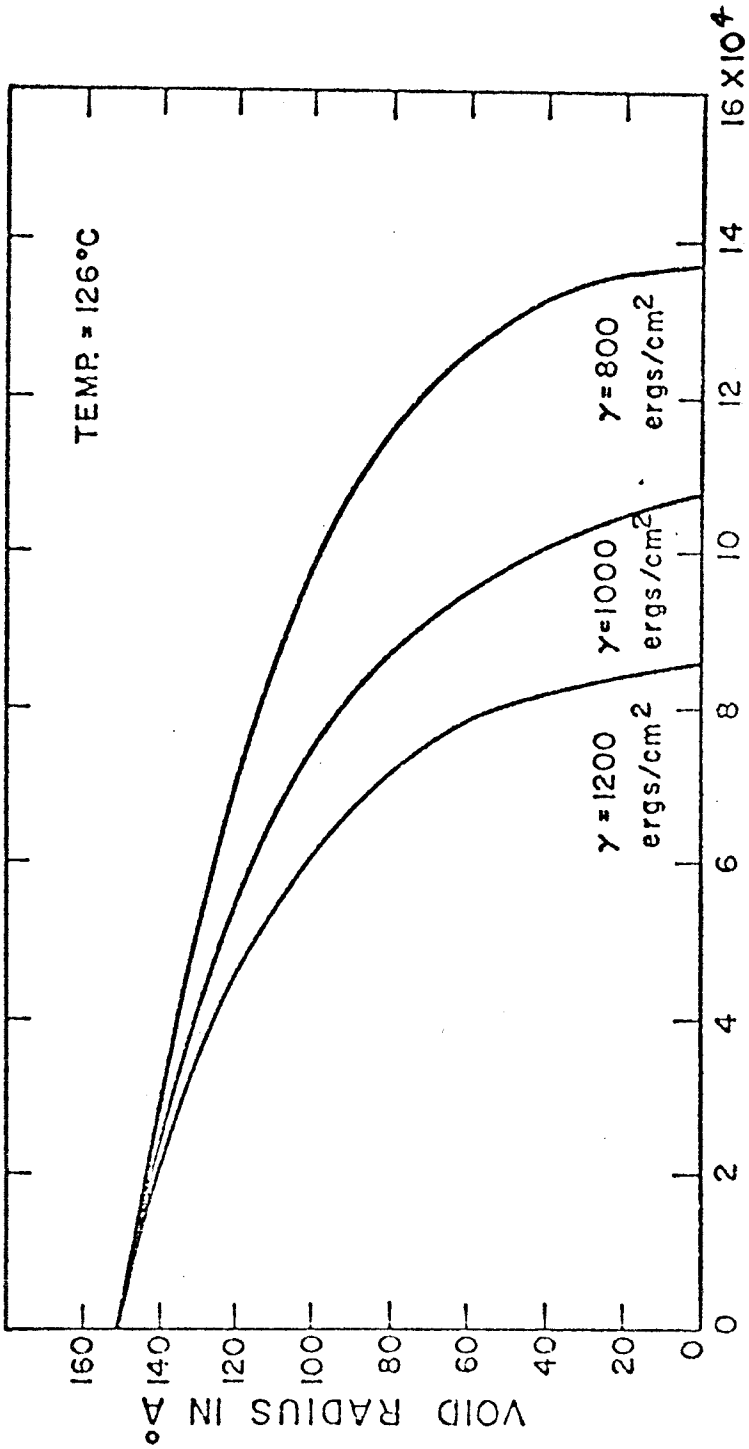

SENSITIVITY OF VOID ANNEALING KINETICS IN ALUMINUM TO SURFACE ENERGY.

FIG. 3

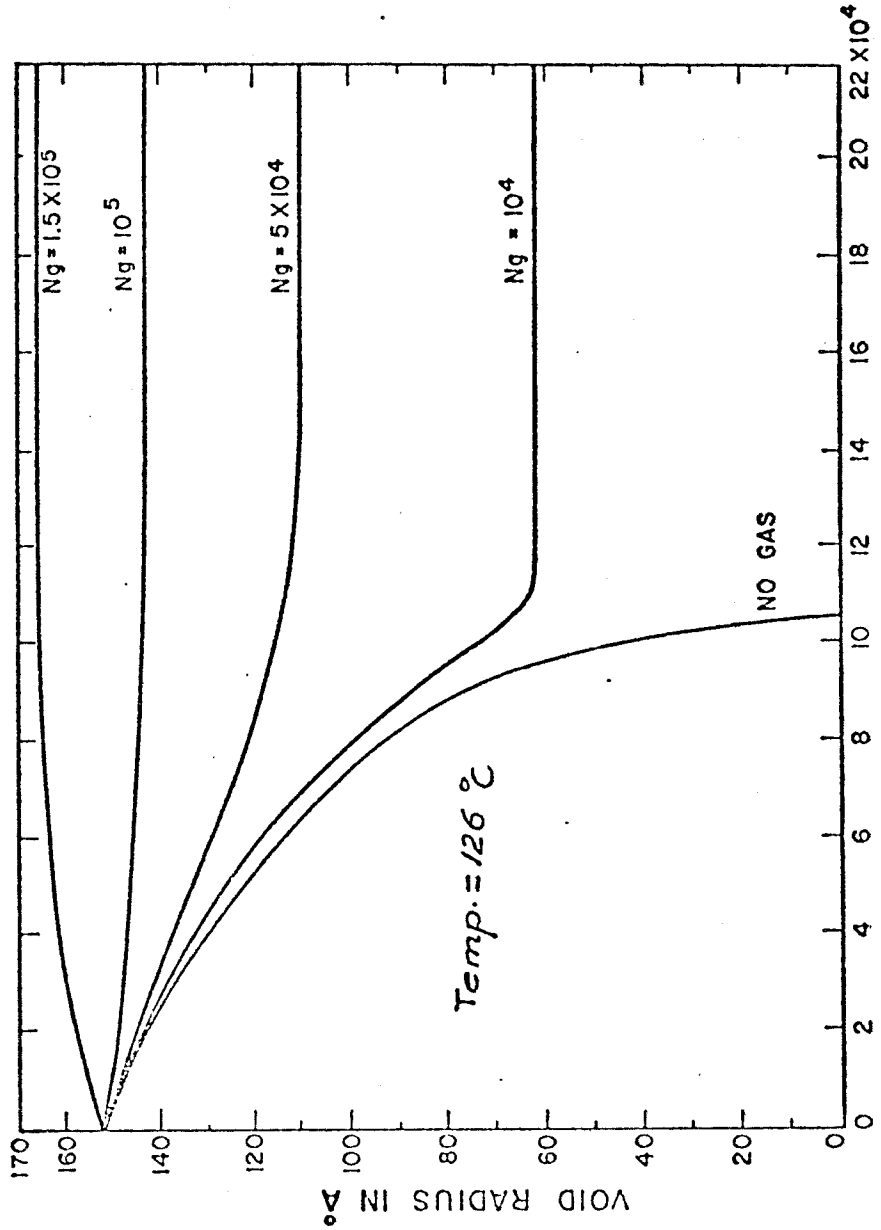

EFFECT OF NUMBER OF He GAS ATOMS IN THE VOID (Ng) ON THE ANNEALING KINETICS OF VOIDS IN ALUMINUM.

FIG. 4

A longer time is needed for the cavity to come to its equilibrium radius as the number of gas atoms is increased. If the number of gas atoms in a cavity is greater than the equilibrium value for this particular radius, it becomes an overpressurized gas bubble. In the case of having 1.5×10^5 He gas atoms in a 152 $\mathring{A}$ radius cavity, such a situation is created. The vacancy concentration at the cavity surface is lower than that of the metal matrix. This creates a flow of vacancies from the matrix to the void relieving the internal gas pressure and the gas bubble grows as shown in figure (4).

VI. Microstructural Impact on Void Annealing

The previous analysis indicated that void annealing kinetics can be substantially altered by different material parameters. The analysis was based on the existence of surfaces that maintain a thermal equilibrium vacancy concentration such as straight dislocations, grain boundaries or specimen flat surfaces. This provides enough driving force for voids to lose their vacancies to these surfaces by thermal emission.

In electron irradiation of metals voids and interstitial loops are formed. Besides voids and interstitial loops, heavy ion or neutron irradiation of metals involve the collapse of collision cascades to form vacancy loops. In this section we will concentrate on the effect of existing planar surfaces, interstitial loops, vacancy loops and voids on the annealing behavior of voids.

VI.1. Analysis

If the irradiation is turned off and no irradiation produced point defects exist, the following processes can be analyzed.

Dislocation Densities

$$\rho_d^{i\ell n} = 2\pi r_{i\ell n} N_{i\ell n} \tag{8}$$

$$\rho_d^{i\ell a} = 2\pi r_{i\ell a} N_{i\ell a} \tag{9}$$

$$\rho_d^{v\ell n} = 2\sqrt{\pi N_{v\ell n} Q_{v\ell n}/b} \tag{10}$$

$$\rho_d^{v\ell a} = 2\sqrt{\pi N_{v\ell a} Q_{v\ell a}} \tag{11}$$

$$\rho_d = \rho_d^e + \rho_d^{i\ell n} + \rho_d^{i\ell a} + \rho_d^{v\ell n} + \rho_d^{v\ell a} \tag{12}$$

where,

- $\rho_d^{i\ell n}$ is the non-aligned dislocation loop line density; cm^{-2}.
- $N_{i\ell n}$ is the non-aligned dislocation loop concentration; cm^{-3}.
- $\rho_d^{i\ell a}$ is the aligned dislocation loop line density; cm^{-2}.
- $N_{i\ell a}$ is the aligned dislocation loop concentration; cm^{-3}.
- $\rho_d^{v\ell n}$ is the non-aligned vacancy loop line density; cm^{-2}.
- $\rho_d^{v\ell a}$ is the aligned vacancy loop line density; cm^{-2}.
- ρ_d^{e} is the deformation produced edge dislocation line density; cm^{-2}.
- ρ_d is the total dislocation line density produced by both deformation and radiation; cm^{-2}.
- $r_{i\ell n}$ is the non-aligned dislocation loop radius; cm.
- $r_{i\ell a}$ is the aligned dislocation loop radius; cm.
- $N_{v\ell n}$ is the non-aligned vacancy loop concentration; cm^{-3}.
- $N_{v\ell a}$ is the aligned vacancy loop concentration; cm^{-3}.
- $Q_{v\ell n}$ is the fraction of vacancies tied up in non-aligned vacancy loops; at/at.
- $Q_{v\ell a}$ is the fraction of vacancies tied up in aligned vacancy loops; at/at.

Vacancy Emission From Voids

$$p_c^e = 4\pi R_c N_c D_v C_v^e \exp\{(\frac{2\gamma}{R_c} - P_g(R_c, N_g))\Omega/kT\} \qquad (13)$$

where

- P_c^e is the vacancy emission rate from the surface of all voids, s^{-1}
- N_c is the temperature dependent void concentration, cm^{-3}
- D_v is the temperature dependent vacancy diffusion coefficient, $cm^2\ s^{-1}$
- C_v^e is the equilibrium vacancy concentration, at./at.
- γ is the surface energy of the void surface, eV/cm^2
- P_g is the gas pressure inside the void, eV/cm^3
- N_g is the number of gas atoms in a void.

Vacancy Emission from Deformation Produced Dislocations

$$P_d^{ea} = Z_v^a D_v C_v^e \exp(\sigma\Omega/kT)\ \rho_d^{ea} \tag{14}$$

$$P_d^{en} = Z_v^n D_v C_v^e\ \rho_d^{en} \tag{15}$$

$$P_d^e = P_d^{ea} + P_d^{en} \tag{16}$$

where

- P_d^{ea} is the rate of vacancy emission from all aligned edge dislocations, s^{-1}
- P_d^{en} is the rate of vacancy emission from all non-aligned edge dislocations, s^{-1}
- P_d^e is the total rate of vacancy emission from edge dislocations

- σ is the uniaxial externally applied stress, eV/cm^3
- Ω is the atomic volume, cm^3
- k is Bolzmann's constant, $eV\ ^oK^{-1}$
- ρ_d^{ea} is the aligned edge dislocation density, cm^{-2}
- ρ_d^{en} is the **non-aligned** edge dislocation density, cm^{-2}
- Z_v^a is the vacancy-aligned dislocation bias factor
- Z_v^n is the vacancy non-aligned dislocation bias factor
- T is the temperature, ^oK

Vacancy Emission from Interstitial Loops

$$P_d^{i\ell a} = D_v C_v(r_{i\ell a}) Z_v^a \exp(\sigma\Omega/kT)\ \rho_d^{i\ell a} \tag{17}$$

$$P_d^{i\ell n} = D_v C_v(r_{i\ell n}) Z_v^n\ \rho_d^{i\ell n} \tag{18}$$

$$P_d^{i\ell} = P_d^{i\ell a} + P_d^{i\ell n} \tag{19}$$

$$C_v(r_{i\ell}) = C_v^e \exp - \left(\frac{\{\gamma_{sf} + F_{el}(r_{i\ell})\} b^2}{kT} \right) \tag{20}$$

$$F_{el}(r_{i\ell}) = \frac{\mu b^2}{(1-\nu) 4\pi r_{i\ell} + b} \ell n \left(\frac{r_{i\ell} + b}{b} \right) \tag{21}$$

where

- $P_d^{i\ell a}$ is the rate of vacancy emission from aligned interstitial loops, s^{-1}
- $P_d^{i\ell n}$ is the rate of vacancy emission from non-aligned interstitial loops, s^{-1}
- $P_d^{i\ell}$ is the total rate of vacancy emission from all interstitial loops, s^{-1}
- γ_{sf} is the stacking fault energy, eV cm^{-2}
- $F_{el}(r_{i\ell})$ is the elastic energy of a dislocation loop of radius $(r_{i\ell})$, eV cm^{-2}
- b is the Burger's vector, cm
- μ is the shear modulus, eV cm^{-3}
- ν is the Poisson's ratio
- In (20), $C_v(r_{i\ell})$ is the equilibrium vacancy concentration at the edge of a dislocation loop of radius $r_{i\ell}$.

Vacancy Emission from Vacancy Loops

$$P_d^{v\ell a} = D_v C_v(r_{v\ell}^a) Z_v^a \exp(\sigma\Omega/kT)\, \rho_d^{v\ell a} \tag{22}$$

$$P_d^{v\ell n} = D_v C_v(r_{v\ell}^n) Z_v^n \rho_d^{v\ell n} \tag{23}$$

$$P_d^{v\ell} = P_d^{v\ell a} + P_d^{v\ell n} \tag{24}$$

$$r^{n}_{v\ell} = \sqrt{Q_{v\ell n}/\pi b N_{v\ell n}} \tag{25}$$

$$r^{a}_{v\ell} = \sqrt{Q_{v\ell a}/\pi b N_{v\ell a}} \tag{26}$$

$$C_v(r_{v\ell}) = C^{e}_{v} \exp\left\{\frac{\{\gamma_{sf}+F_{el}(r_{v\ell})\}b^2}{kT}\right\} \tag{27}$$

and $F_{el}(r_{v\ell})$ is as defined in (21) before

where

- $P^{v\ell a}_{d}$ is the rate of vacancy emission from aligned vacancy loops, s-1
- $P^{v\ell n}_{d}$ is the rate of vacancy emission from non-aligned vacancy loops, s^{-1}
- $P^{v\ell}_{d}$ is the total rate of vacancy emission from all vacancy loops, s^{-1}
- $r^{a}_{v\ell}$ is the aligned vacancy loop radius, cm
- $r^{n}_{v\ell}$ is the non-aligned vacancy loop radius, cm
- $\rho^{v\ell a}_{d}$ is the aligned vacancy loop line dislocation density, cm^{-2}
- $\rho^{v\ell n}_{d}$ is the non-aligned vacancy loop line dislocation density, cm^{-2}

Total Rate of Vacancy Emission

$$P^{e} = P^{e}_{V} + P^{e}_{d} + P^{e}_{v\ell} + P^{e}_{i\ell} \tag{28}$$

where P^{e} is the total vacancy emission rate, s^{-1}.

Single Point Defect Time Constants

$$\lambda_i = \lambda^{d}_{i} + \lambda^{c}_{i} \tag{29}$$

$$\lambda_v = \lambda^{d}_{v} + \lambda^{c}_{v} \tag{30}$$

$$\lambda_i^d = \rho_d D_i Z_i \tag{31}$$

$$\lambda_i^c = 4\pi N_c R_c D_i \tag{32}$$

$$\lambda_v^d = \rho_d D_v Z_v \tag{33}$$

$$\lambda_v^c = 4\pi N_c R_c D_v \tag{34}$$

where $\cdot\lambda_i$ is the total single interstitial time constant, s^{-1}

$\cdot\lambda_v$ is the total single vacancy time constant, s^{-1}

$\cdot\lambda_i^d$ is the single interstitial time constant due to all dislocations, s^{-1}

$\cdot\lambda_i^c$ is the single interstitial time constant due to all voids, s^{-1}

$\cdot\lambda_v^d$ is the single vacancy time constant due to all dislocations, s^{-1}

$\cdot\lambda_v^c$ is the single vacancy time constant due to all voids, s^{-1}

Removal Rates

$$P_{si} = \lambda_i C_i \tag{35}$$

$$P_{sv} = \lambda_v C_v \tag{36}$$

$$P_r = \alpha C_i C_v \tag{37}$$

$$\alpha = g\,(\nu_i \exp(-E_i^m/kT) + \nu_v \exp(-E_v^m/kT)) \tag{38}$$

where

$\cdot P_{si}$ is the total sink removal rate for interstitials, s^{-1}

$\cdot P_{sv}$ is the total sink removal rate for vacancies, s^{-1}

- P_r is the total recombination rate of vacancies and interstitials, s^{-1}
- α is the recombination coefficient, s^{-1}
- g is the combinatorial number
- $\nu_i \exp(-E_i^m/kT)$ is the interstitial jump frequency, s^{-1}
- $\nu_v \exp(-E_v^m/kT)$ is the vacancy jump frequency, s^{-1}

Thermal Equilibrium

When irradiation is turned off, as in post irradiation annealing experiments, or in the annealing mode of voids in between pulses, thermal vacancies are emitted from different components of the microstructure and absorbed by others. If the time between pulses is longer than a vacancy mean lifetime, or in a post irradiation annealing experiment, a simple point defect balance situation can be described. Since thermal emission of interstitials from microstructures has a low probability (because of the large interstitial formation energy), then a balance equation for vacancies can be described as:

Total rate of thermal vacancy emission = total rate of vacancy removal

Since thermal concentration of interstitials is very low under these circumstances, vacancy removal by mutual recombination is negligible, and the previous balance equation can be written as:

$$P^e = P_{sv} = \lambda_v \bar{c}_v \ . \tag{39}$$

Now from the previous set of equations the average vacancy concentration $\bar{c}_v$ can be determined as:

$$\bar{c}_v = \frac{p^e}{\lambda_v}, \text{ or} \tag{40}$$

$$\bar{c}_v = c_v^e \left\{ \frac{4\pi R_c N_c \exp\{(\frac{2\gamma}{R_c} - P_g)\frac{\Omega}{kT}\} + Z_v^a \rho_d^{ea} \exp(\sigma\Omega/kT) + Z_v^n \rho_d^{en} + }{4\pi R_c N_c + Z_v^a \rho_d^{ea} + Z_v^n \rho_d^{en} +} \right.$$

$$\frac{Z_v^a \rho_d^{i\ell a} \exp(\sigma\Omega/kT) \exp(-\frac{\{\gamma_{sf} + F_{e\ell}(r_{i\ell}^a)\}b^2}{kT}) + Z_v^n \rho_d^{i\ell n} \exp(-\frac{\{\gamma_{sf} + F_{e\ell}(r_{i\ell}^n)\}b^2}{kT}) +}{Z_v^a \rho_d^{i\ell a} + Z_v^n \rho_c^{i\ell n} +}$$

$$\left. \frac{Z_v^a \rho_d^{v\ell a} \exp(\sigma\Omega/kT) \exp(\frac{\{\gamma_{sf} + F_{e\ell}(r_{v\ell}^a)\}b^2}{kT}) + Z_v^n \rho_d^{v\ell n} \exp(\frac{\{\gamma_{sf} + F_{e\ell}(r_{v\ell}^n)\}b^2}{kT})}{Z_v^a \rho_d^{v\ell a} + Z_v^n \rho_d^{v\ell n}} \right\} \tag{41}$$

VI.2. Discussion and Results

Equation (41) shows that the average thermal vacancy concentration is a function of the microstructure and stress. The annealing of voids depends on the vacancy concentration gradient between the surface of the void and the average thermal vacancy concentration in the matrix. This gradient is proportional to the difference in concentrations as shown in figure (5). According to this schematic representation we have one of 5 different situations:

Case	Average Thermal Vacancy Concentration
1. Edge dislocations on specimen surfaces only	c_v^e
2. Small interstitial loops only	$c_v^e \exp\{-(F_{e\ell}+\gamma_{sf})\frac{b^2}{kT}\}$
3. Small voids only	$c_v^e \exp(\frac{2\gamma}{R_c} - p)$
4. Small vacancy loops only	$c_v^e \exp\{+(F_{e\ell}+\gamma_{sf})\frac{b^2}{kT}\}$
5. A mixed microstructure	$\bar{c}_v$

It is demonstrated in figure (5) that vacancy loops help voids to grow while interstitial loops make them shrink faster.

The geometry factors (the ratios between vacancy concentrations at the edge of a particular microstructure to C_v^e) are plotted in figure (6) for voids, vacancy loops and interstitial loops as a function of radius. It is shown that the void geometry factor (with no gas pressure inside) is a very sensitive function of the radius and approaches the value 1.00 for large radii. This has the implication that large voids anneal out much slower than small voids. The geometry factor for a vacancy loop is less sensitive to its radius and is controlled by the stacking fault energy for large radii. The interstitial loop geometry factor is less than 1.00, being close to zero for small radii and approaching a value of about 0.17 for very large radii as controlled by the stacking fault energy.

To study the effect of changing the microstructure on the annealing of voids, the number of voids was fixed to 10^6 voids/cm^3 and their radius to 152 $\mathring{A}$. An equivalent number of interstitials to that of vacancies in the voids was distributed on interstitial loops. The only variable in the calculations was the ratio of interstitial loops to voids ranging from 10^{-6} to 10^4 with a negligible concentration of straight edge dislocations. It is evident from figure (7) that voids anneal out much faster for larger ratios while their annealing kinetics become slow when voids are the dominant thermal vacancy source/sink.

VII. Conclusions

The annealing behavior of voids in aluminum was analyzed in this paper in detail because of the importance of this behavior in determining the response

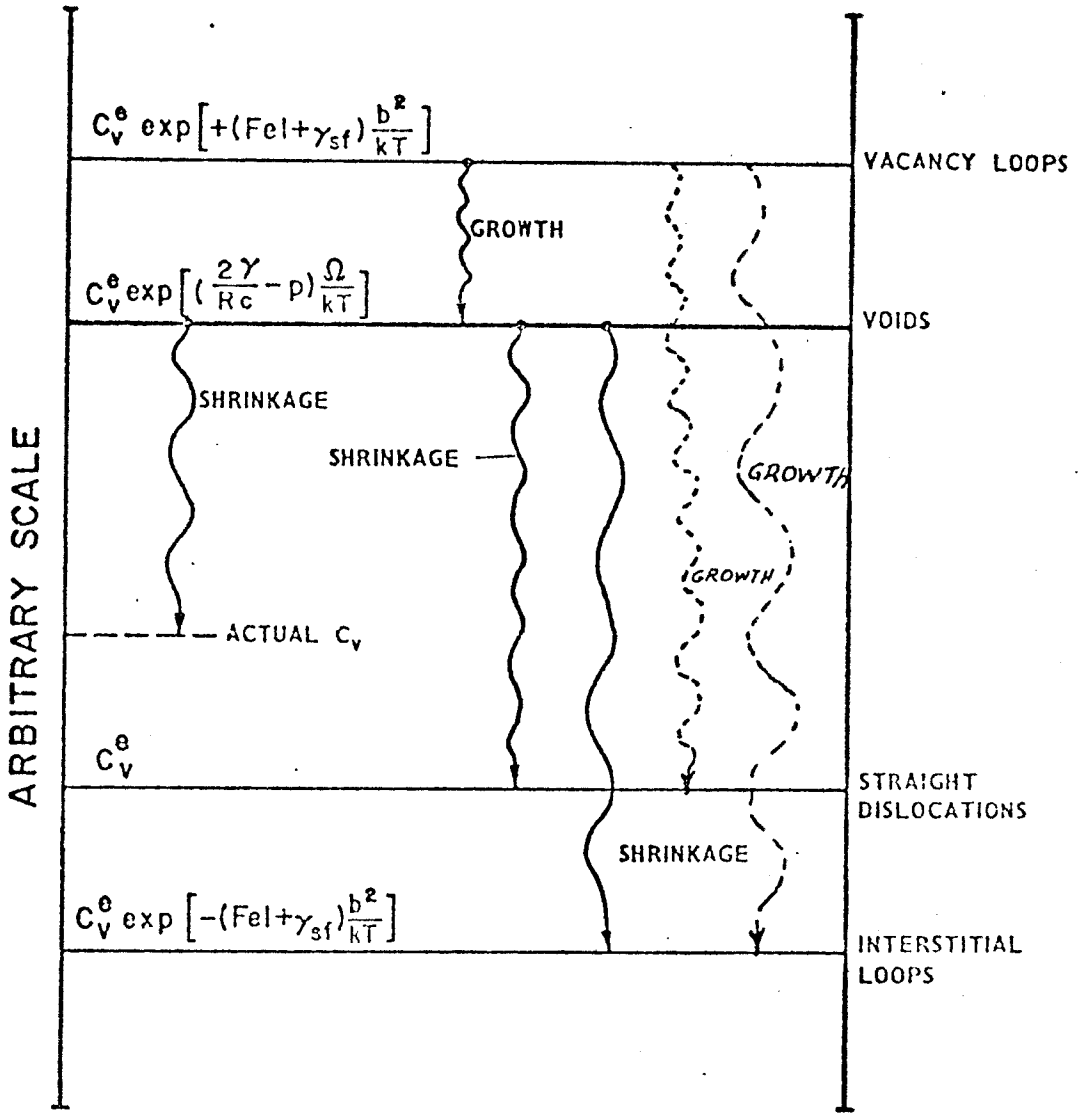

FIG. 5 Schematic illustration of main thermal annealing kinetics and their relation to microstructure.

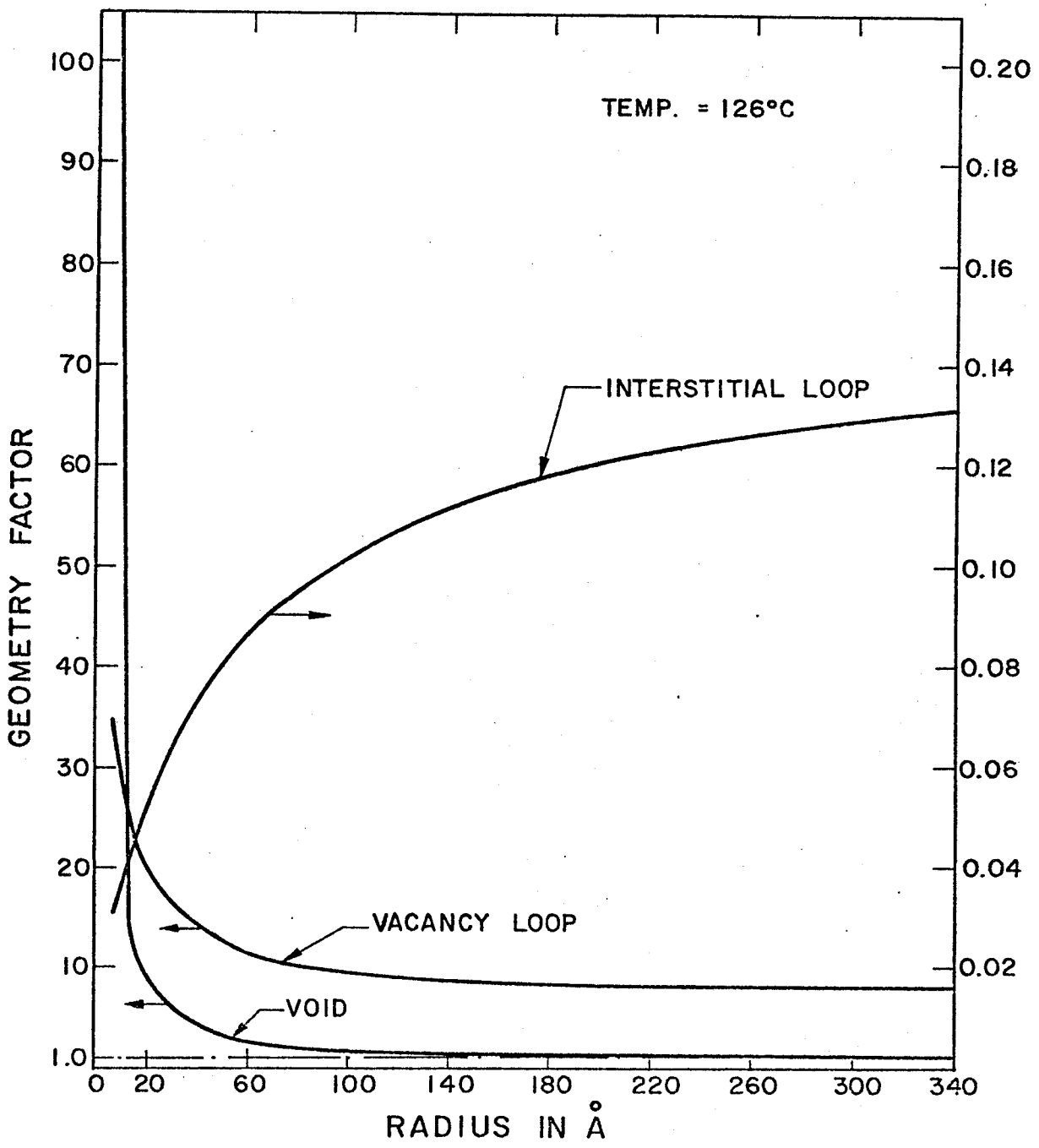

FIG. 6 GEOMETRY FACTORS FOR VOIDS, INTERSTRAL LOOPS AND VACANCY LOOPS AS A FUNCTION OF RADIUS.

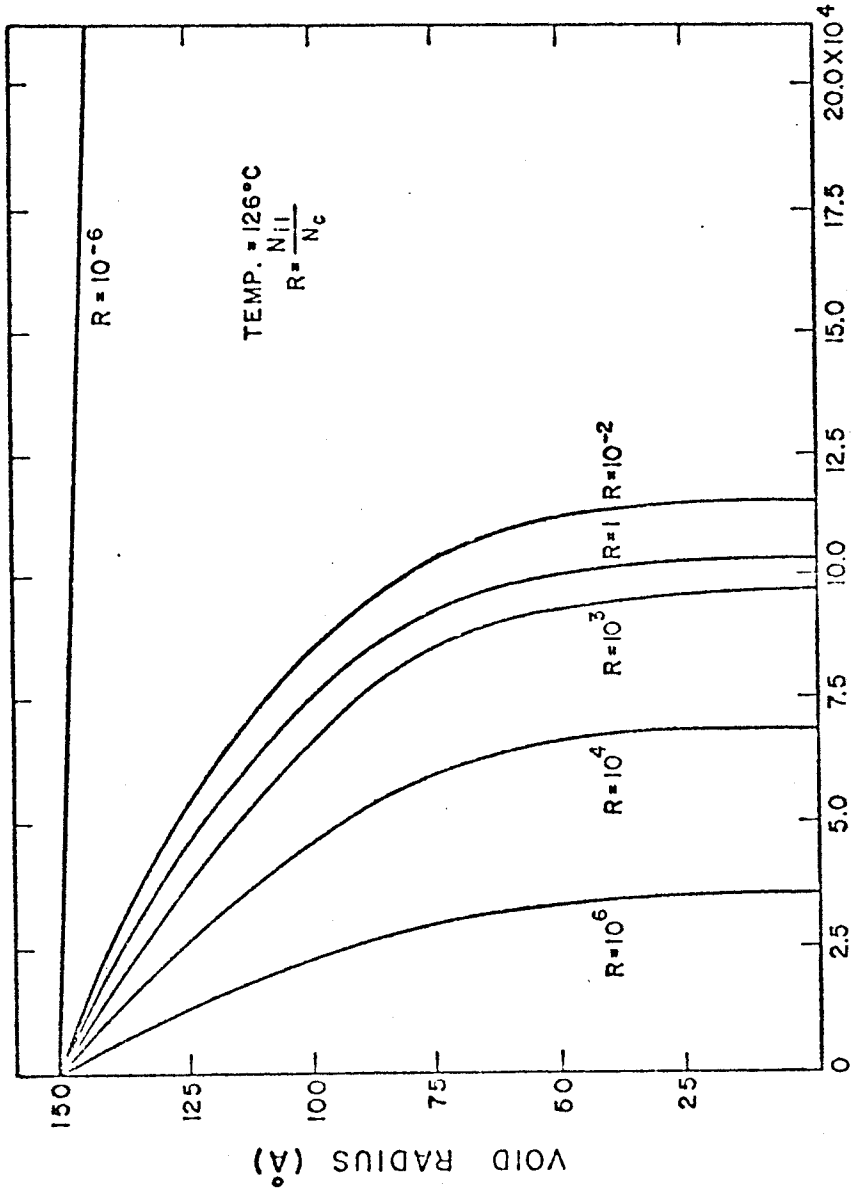

EFFECT OF RATIO OF INTERSTITIAL LOOPS TO VOIDS ON ANNEALING OF VOIDS IN ALUMINUM.

FIG. 7

of metals to pulsed irradiation. The previous analysis indicates the following:

1. The bulk diffusion model is successful in predicting the annealing behavior of voids in metals. In aluminum, a surface energy of 1000 ergs/cm^2 and vacancy formation energy between 0.645 and 0.665 eV were established. The higher value of E_v^f at the higher temperature is due to neglecting divacancies in the kinetics.[8]

2. Annealing of voids is enhanced if one or more of the following conditions is satisfied:

(a) High temperature; (b) small void radius; (c) large void surface energy; (d) no gas content; (e) high density of deformation produced dislocations; and (f) high concentration of small interstitial loops.

3. Annealing of voids is retarded by one or a combination of the following conditions:

(a) Low temperature; (b) large void radius; (c) small void surface energy; (d) the presence of gas atoms inside the void; (e) low density of deformation produced dislocations; (f) interstitial loops that are few in number density and large in size; and (g) a large number of small vacancy loops.

References

1. S.D. Harkness and Che-Yu Li, Proc. of International Conf. on Voids, Albany, Ed., L.W. Corbett, (1971), P. 798.

2. A.D. Brailsford and R. Bullough, J. Nucl. Mater., 44 (1972), P. 121.

3. N. Ghoniem and G.L. Kulcinski, Fully Dynamic Rate Theory (FDRT) Simulation of Radiation Induced Swelling of Metals, October, 1976.

4. N. Ghoniem and G.L. Kulcinski, TRANSWELL (Version I) Computer Code Documentation, October, 1976.

5. T.E. Volin and T.W. Balluffi, Phys. Stat. Vol. 25, 163, (1968).

6. K.H. Westmacott, R.E. Smallman, and P.S. Dobson, Metals Science Journal, Vol. 2, (1968), P. 177.

7. Westmacott, to be published.

8. P. Wilkes, Personal Communications.